communications earth & environment

Article

A Nature Portfolio journal

https://doi.org/10.1038/s43247-026-03184-w

Climate change and ocean acidification pose a risk to underwater cultural heritage

Luigi Germinario [1] ✉, Marco Munari[2,3], Isabella Moro[2,3], David Benavente[4], Francesco Terlizzi[5] & Claudio Mazzoli [1]

Ocean acidification caused by climate change drives a spectrum of ecological impacts on the marine environment, while also posing a lurking threat to the traces of human history lying on seabeds. We present a quantitative assessment of the climate change risk to underwater cultural heritage, focusing on the vulnerability of historical stone materials to shifting ocean pH levels. We monitored the amount and rate of stone surface material loss and textural alteration triggered by natural processes of mineral dissolution and biodeterioration in submarine settings, combining field and laboratory experimentations with climate models. Stone deterioration has been minimal in pre-industrial and present times; however, escalating anthropogenic emissions might lead to an exponential surge in vulnerability, with irreversible decay processes accelerating in the next decades and centuries, constrained by material properties and shifting biofouling dynamics. Ocean acidification will dramatically challenge the protection of underwater cultural heritage, demanding urgent preservation and adaptation policies.

Oceans and seas represent major regulators of global climate systems, controlling the water cycle, moderating and stabilizing temperatures, redistributing heat, and acting as carbon sinks[1]. Their environmental balance is being almost irreversibly disrupted by anthropogenic climate change[2], in particular by increasing ocean temperature, acidification, deoxygenation, surface level, and extreme events[3,4]. Ocean acidification is driven by the uptake of the escalating amounts of CO_2 emitted by human activities into the atmosphere. Since the pre-industrial period, seawater acidity has increased by at least ~30% and will possibly be threefold by the end of this century[3,5]. The related pH reduction and changes of carbonate chemistry endanger marine ecosystems and indirectly human communities, paving the way to a severe loss of biodiversity and decline of fishery and aquaculture[6,7]. These threats are mainly connected with the changing physiology of marine life, especially the enhanced vulnerability of calcifying organisms like corals, coralline algae, and phytoplankton[8,9]. Previous research has mainly addressed the ecological, socioeconomic, and health impacts, but an "invisible" domain has been largely neglected, that of underwater cultural heritage and its historical legacy, which includes millions of submerged historical settlements, wrecks, artifacts, and structures worldwide[10], some related to World Heritage Sites[11]. This shortcoming is noticeable in early reference documents (such as the UNESCO Convention[12]) as well as the latest IPCC reports (containing only few brief mentions about shipwreck vulnerability[8,13]). Considering submarine cultural assets, speculations have been formulated on their increasing corrosion and changing biofouling due to ocean warming, acidification, and salinity alteration, or their erosion and displacement from stronger storms, waves, and currents[14–18]. However, the climate change impacts have never been quantified or modeled, with most attention being rather devoted to coastal sites, sea level rise, coastal flooding, and erosion. This reflects a delay compared to the lively debate around terrestrial cultural heritage, which spans over twenty years[19–23].

Aiming to bridge that gap, this paper presents a quantitative assessment of the ocean acidification risk to underwater cultural heritage, with a focus on stone materials; these are among the most important natural resources used in human history and prehistory and part of countless submerged remains of ancient buildings, harbors, roads, sculptures, tools, and ship cargoes. This interdisciplinary study simulates and predicts the effects of ocean acidification by monitoring the amount and rate of stone decay across a range of past, present, and future ocean pH levels, through an innovative mixed field and laboratory experimentation. Stone changes were quantified during one-year exposure tests at different pH levels, under natural conditions at submarine CO_2 vent sites (with underwater exposure setups—UES) and under controlled laboratory conditions (with a prototype MicroEnvironment Simulator—MES). The experimental data were finally combined with historical and future climate models.

[1]Department of Geosciences, University of Padova, Padova, Italy. [2]Department of Biology, University of Padova, Padova, Italy. [3]Department of Integrated Marine Ecology, Zoological Station Anton Dohrn, Naples, Italy. [4]Department of Earth and Environmental Sciences, University of Alicante, Alicante, Spain. [5]Department of Research Infrastructures for Marine Biological Resources, Zoological Station Anton Dohrn, Naples, Italy. ✉e-mail: luigi.germinario@gmail.com

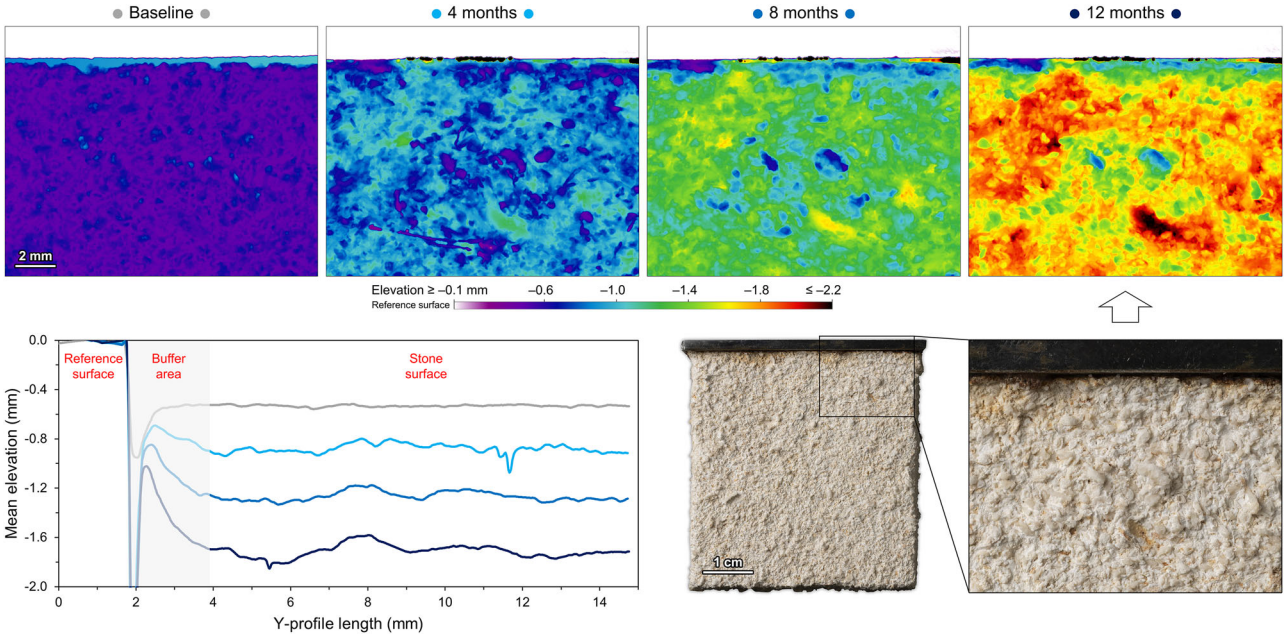

Fig. 1 | 3D modeling of stone surface evolution. False-color 3D models of a porous limestone specimen and their average topographic trends at different monitoring steps, showing the surface time evolution in the UES extreme acidification site.

Results and discussion

Surface changes: material loss

This research focuses on carbonate rocks, on account of their historical significance and extensive use worldwide, besides their vulnerability to ocean acidification, which drives the increasing solubility of $CaCO_3$ minerals and dissolution rate. The underwater decay of the stone samples selected as representative historical materials (see "Methods" and Supplementary Fig. 1) can first be discussed based on the amount and rate of surface material loss caused by calcite dissolution at different pH levels (an example in Fig. 1). The annual material loss data, both directly measured in the UES field tests and extrapolated in the MES laboratory tests, will be presented together, in order to capture the typical variability of stone erosion evolution. On the one hand, erosion in natural conditions tends to be comparatively stronger, being influenced by wave motion, currents, and sediment transport; biodeterioration and natural pH fluctuations also come into play[24,25]. On the other hand, the static semi-closed environment of the laboratory simulations involves higher pH stability and more reproducible data, although excluding the natural oceanic processes and water recirculation.

At pH levels of 8.2–8.1 (simulating pre-industrial and current ocean settings), surface erosion is hardly measurable for marble, travertine, and compact limestone, being often less than or equal to 1 µm/yr, while falling between 9 and 49 µm/yr on average for porous limestone. At decreasing pH levels of 7.8–7.5 (simulating future ocean acidification settings linked to very high anthropogenic emissions), average material loss is 1 µm/yr for marble, 9 µm/yr for travertine and compact limestone, and 15–90 µm/yr for porous limestone. Even lower pH levels (simulating low-likelihood and far-future extreme acidification settings) are associated with an abrupt enhancement of erosion processes: at pH 7.0, average surface recession is 11 µm/yr for marble, 48 µm/yr for travertine, 79 µm/yr for compact limestone, and 304 µm/yr for porous limestone; at pH 6.8, it reaches 253, 314, 394, and 1248 µm/yr, respectively. The distinct erosion data for each stone sample and pH value are enclosed as Supplementary Data 1 (also indirectly validated by the measures of bulk weight loss in the Supplementary Data 2).

The regression analysis describes how material loss increases exponentially with decreasing pH and linearly with time (Fig. 2). The exponential models are valid for 20 °C but can be adjusted to other temperatures, also in light of ocean warming, considering that as temperature rises, calcite solubility decreases but dissolution rate increases[26,27]; moreover, the models apply to shallow water environments but also accounting for sea level rise, since pressure notably increases calcite solubility only at depths of hundreds or thousands of meters[27,28]. Regarding time evolution, linearity is well described by the UES erosion trends and their coefficients of determination (Supplementary Data 1; an example in Fig. 2). This is consistent with the literature describing steady-state dissolution rates in seawater after a short, initial non-linear and more rapid phase[26,27,29]. It also corroborates the extrapolations done for the MES data or for filling the gaps in the UES data series.

Another point to address is the difference between the exposed (front) and shielded (back) surfaces of the stone specimens in the UES experiments. In the extreme acidification site, erosion is slower for the shielded surfaces, which are much less influenced by wave, current, and sediment movements or seawater recirculation (the water layers and calcium ions released from dissolution are more stationary, leading to a more alkaline and less corrosive state); this is confirmed by the differential erosion of the (more exposed) edges of the shielded surfaces, which can be even 1.5–2 times higher for marble, travertine, and compact limestone. The trends in the UES ambient pH site and acidification site are often opposite: pH is much higher and close to the equilibrium there; moreover, the encrusting biofouling on the exposed surfaces may constitute a thin protective barrier.

Besides the pH levels, the diverse behavior exhibited by the stone materials is controlled by their textural and technical properties, in particular calcite grain size and open porosity, which also affects specific surface area and mechanical strength (Supplementary Fig. 1). Marble first, and then travertine and compact limestone are the most resistant to surface changes, all sharing high mechanical strength and limited capillary- and microporosity: that implies stronger intercrystalline bonds and resistance to disintegration, as well as restrained processes of water intrusion and in-pore movement; however, dissolution is more intense for compact limestone, because of the much finer grain size and higher active surface area[26,30]. On the opposite side, porous limestone shows by far the strongest decay in the entire set. The considerations about grain size effects are corroborated by the differential erosion patterns observed: the coarser calcite cement in travertine and compact limestone (in vugs and fractures) recedes more slowly, as bioclasts do in porous limestone (raising in relief above the finer matrix). In marble, differential erosion is controlled not by grain size—which is homogeneous—but by crystallographic orientations in the calcite mosaic[31].

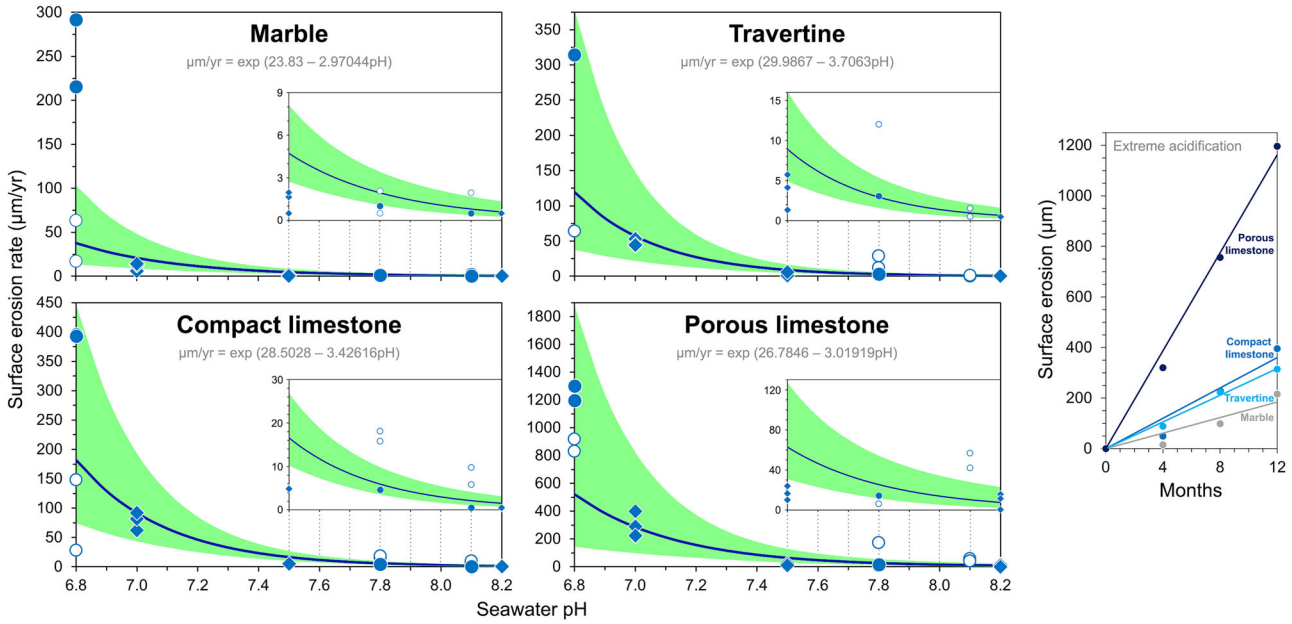

Fig. 2 | Stone surface material loss. Surface erosion at different seawater pH levels, indicated by the experimental data points (solid circles = UES exposed; open circles = UES shielded; diamonds = MES), their fitted exponential trends and functions (obtained excluding the shielded surfaces in the UES extreme acidification site), and the 95% confidence bands (in green). The small plot shows an example of the temporal linearity of erosion in the extreme acidification site.

Surface changes: textural alteration and biodeterioration

A complementary perspective is provided by the patterns of stone textural changes, which can be reviewed by distinguishing between clean and biofouled surfaces, thus also considering the stone biodeterioration occurred during the UES monitoring (complete dataset in Supplementary Data 1).

Starting with the clean surfaces (i.e., biofouling-free due to shielding or the very low pH), Fig. 3 shows a comparison of four representative morphometric parameters: root-mean-square (RMS) roughness, maximum peak height, surface slope, and surface area-to-area ratio (SAAR). The general trend indicates their increase with time and seawater acidification, describing a growing surface irregularity, more marked on the exposed (front) surfaces. Good temporal linearity is shown only by RMS roughness. Textural alteration becomes more pronounced along the sequence marble, compact limestone, travertine, and porous limestone, similarly to material loss. The UES ambient pH site and acidification site are comparable: for instance, the annual variation of RMS roughness in both sites ranges mostly between 0 and 2 μm, but travertine and porous limestone record maxima of around 20 μm. Much larger variations characterize the UES extreme acidification site: the annual increase of RMS roughness may reach 37 μm for marble, 58 μm for compact limestone, 83 μm for travertine, and 178 μm for porous limestone. Another brief example in the same UES site is provided by porous limestone and its SAAR annual increase of about 20%, which instead does not exceed 3% elsewhere. These trends are confirmed by the MES experiments (with smaller changes), which point out the most significant surge in textural alteration at pH 7.0.

Finally, examining the biofouled surfaces, it is clear that biodiversity progressively diminishes as seawater acidification increases. Stone biofouling in the ambient pH site is represented, for the calcifying colonies, mainly by barnacles (Balanidae), tubeworms (Serpulidae), red algae (Corallinales), and bryozoans (*Schizoporella*); the non-calcifying colonies include filamentous brown, green, and red algae (Phaeophyceae, Chlorophyceae, and Rhodophyceae), besides diatoms. In the acidification site, biofouling is dominated by tubeworms and calcareous red algae, with barnacles and bryozoans almost disappearing, besides soft red, green, and brown algae. No noteworthy encrusting biocolonization was observed in the extreme acidification site, where stone surfaces are covered only with soft filamentous algae. The encrusting colonies are the main responsible for the greatest and irreversible textural alterations (Fig. 3). With respect to the initial state, the encrusting biofouling developed in one year is associated with a general average increase of RMS roughness by 288 μm at ambient pH and by 139 μm in acidified conditions. Considering maximum peak height, which is a parameter very sensitive to topographic outliers, its average increases are 1602 μm at ambient pH and 766 μm in acidified conditions. The higher values at ambient pH are mainly connected to the diffuse growth of barnacles, which can frequently reach a centimetric size.

Modeled risk and decay trends

The experimental models describing stone surface changes were combined with the IPCC data of ocean pH, in order to define decay trends for underwater cultural heritage and assess its risk in pre-industrial, present, future, and far future periods. The trends do not include biofouling and are material-specific; however, given the spectrum of textures and technical properties considered in this study, they can represent a reference for all carbonate rock types.

Figure 4 shows time- and space-based information on the erosion rate of stone heritage, considering the extremes within the IPCC scenarios based on shared socioeconomic pathways (SSPs)[32,33]: SSP1-1.9, the most optimistic, with very low greenhouse gas emissions (declining to net zero by mid-century) and a global warming limited to 1.5 °C; and SSP5-8.5, the most pessimistic, with very high emissions (almost doubling the current levels by mid-century) and a warming exceeding 4.0 °C[2]. In the low-emission scenario, erosion rate is not expected to vary significantly through this century compared to the pre-industrial period, with relative changes never exceeding 1 μm/yr (except for porous limestone, peaking at 5 μm/yr). Over the same period, the high-emission scenario implies much higher deterioration kinetics, which would steeply accelerate after mid-century and finally reach a four- to six-fold increase, from 2 to 30 μm/yr (for the end members marble and porous limestone, respectively). The global maps in Fig. 4 deliver a perspective of how the risk to underwater stone heritage changes in space, other than time. In the pre-industrial era, stone deterioration was generally very limited, with the Arctic region recording the lowest risk. By the end of this century and with high anthropogenic emissions, the risk is expected to raise significantly worldwide, but with a reverse geographic trend, with subpolar and polar regions—those with less tangible cultural heritage—being threatened the most (due to the possible

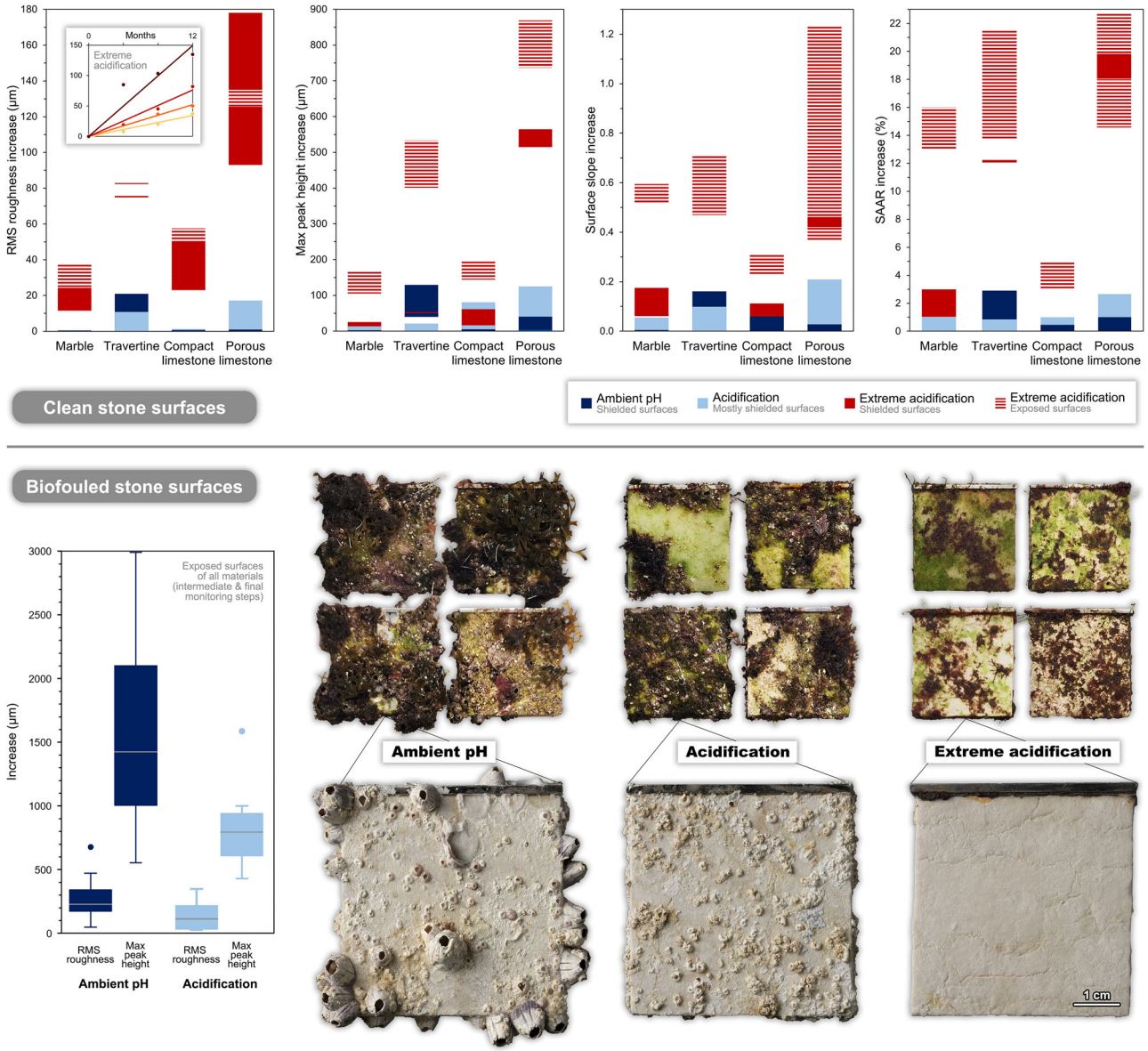

Fig. 3 | Stone textural alteration and biodeterioration. Changes of representative morphometric parameters at different pH levels during the UES experimentation, relative to the initial state. The measurements were taken on: clean surfaces, mostly after the one-year exposure, also including high outliers from intermediate monitoring steps (inset: temporal linearity of increasing RMS roughness for the four stones in the extreme acidification site); and biofouled surfaces, presenting the morphometric analysis of the encrusting biocolonization and a comparison before/after removing all non-calcifying organisms from a representative sample of compact limestone exposed continuously for one year (the other stones are also shown for reference).

combination of increased CO_2 uptake, sea ice melt, and riverine and glacial discharges[3]).

This global risk assessment can be refined at the regional scale by incorporating local seawater pH data. Here, the example of the Mediterranean Sea is considered, given its rich underwater cultural heritage, its status of a climate change hotspot[8], and the location of the UES. The regional acidification trend is very similar to the global trend[33], with only a minimal shift due to the ~5% higher alkalinity of the Mediterranean Sea, so stone erosion rate is expected to be of the same order (Supplementary Fig. 2). However, this stems from basin-wide pH averages; higher-resolution observations indicate that certain sub-basins (e.g., the Western Mediterranean) are experiencing a more rapid acidification[34]. Considering the biodeterioration risk, rising temperatures in the Mediterranean promote the spread of tropical and subtropical species, including fishes, molluscs, crustaceans, and macroalgae, some showing tolerance to low pH. A notable example is the invasive seaweed *Asparagopsis taxiformis*, whose resilience to acidified conditions indicates an enhanced colonization potential on hard substrates in low-competition habitats[35], although some native groups, such as Corallinaceae, may also persist under comparable conditions[36]. Elevated CO_2 may also boost the chemical etching activity of micro- and macroborers, such as Porifera (*Cliona* spp.), Polychaeta, and Sipuncula[37].

In order to support the visualization of the possible damage of actual archeological materials, Fig. 5 shows 3D simulations of deterioration of a Roman marble sculpture from Baia (Italy), one of the most renowned underwater archeological sites in the world. In a time span of 500 years in a hypothetical pre-industrial setting, the artifact would preserve almost entirely its features, with a surface recession of a few hundred µm. At the ocean pH levels expected by the end of this century, a surface loss of over 1 mm would be experienced instead; this means that the very vulnerable fine sculptural details would vanish, together with their artistic value. Finally, a far-future scenario of extreme acidification would entail major disruptions of the general shape and texture of the artifact: its surface would get eroded

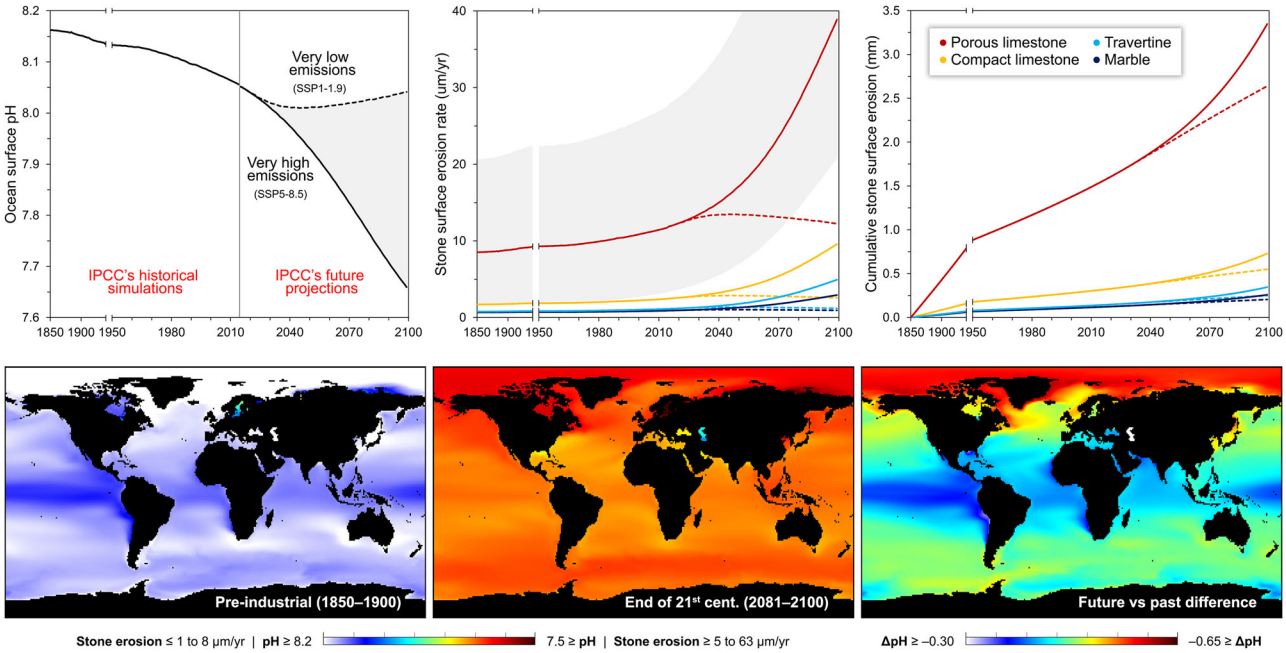

Fig. 4 | Spatiotemporal predictions of stone heritage decay. Temporal stone erosion trends with changing global ocean surface pH, according to the IPCC's historical simulated and future projected data combined with the exponential decay models of this study (Fig. 2), assuming time-dependent linearity, 20 °C temperature, and shallow depth. The plots show the decay trends in two IPCC scenarios, SSP1-1.9 (dashed) and SSP5-8.5 (solid)[32], with an illustrative 95% confidence band of the erosion model for porous limestone. The global maps show the IPCC's CMIP6 models for the pre-industrial period 1850–1900 and the SSP5-8.5 scenario 2081–2100[33], with the corresponding ranges of stone erosion rate (with marble and porous limestone as limits) and the difference of mean annual pH between the future and the past.

by over 1 cm and become much more asperous, with a roughness increase of at least 0.5 mm. It is worth noticing that, under the same conditions, a material with much lower durability like porous limestone could experience a catastrophic erosion from a few cm to over 10 cm during just one century, which would take millennia at pre-industrial or current pH levels. Extreme emission scenarios might in fact entail pH decreases down to 7.5 or even 6.8 by 2300[38–40], but these long-term future projections have a much lower likelihood and reliability.

Conclusions

Anthropogenic climate change and ocean acidification may have a dramatic impact on the survival of underwater cultural heritage and its component stone materials, as suggested by the experimental field and laboratory findings. Stone deterioration driven by natural dissolution processes in the submarine environment has historically proceeded at a slow pace until the present time, with only a modest increase especially from the mid-20th century, caused by escalating greenhouse gas emissions and a faster ocean pH decline. To date, global emissions have yet to peak, and limiting global warming to the 1.5 °C target now seems unlikely, if not out of reach, given the international policies and outcomes of the recent climate COPs. With growing emissions, by the end of this century, underwater stone heritage might experience exponentially-increasing processes of irreversible material loss and textural alteration up to four times faster than today and six times faster than the pre-industrial period. In an even more distant future scenario of uncontrolled emissions (very improbable but not excludable), the stone decay rate might increase by one or even two orders of magnitude; at the same time, with changing biodeterioration and encrusting biofouling gradually disappearing, archeological surfaces will be left with no protective barrier. Generally, the predicted future trend will pose serious challenges to the in-situ protection of historical materials underwater, their features, and cultural legacy.

Despite its applicability limitations (only carbonate materials and pH change as the main driving force), this study is open to several ways of scientific exploitation; not just in heritage science (e.g., for exploring the deterioration of other materials or new conservation methods and products), but also indirectly in disciplines involved in ocean protection, like ecology and geomorphology: for example, dealing with the vulnerability of coral reefs (note: aragonite structures are even more vulnerable than calcite[41]) and other submarine landscapes.

Finally, this research calls for long-term strategies and policies for adaptation and the preservation of underwater cultural heritage, which is often physically inaccessible and perceived as «out of sight and out of mind»[42], but demands awareness of its values and threats and acknowledgment of its diversity (freshwater environments are also involved!).

Methods

Stone selection and characterization

Four materials were designated as representative of the broad spectrum of textures and technical properties that carbonate rocks used in cultural heritage may have[43,44]: marble (Carrara marble), travertine (Roman travertine), compact limestone (Istria stone), and porous limestone (Vicenza stone). Their basic characterization was performed by:

- Polarized-light microscopy on thin section, for achieving the petrographic classification;
- X-ray fluorescence (XRF), by a wavelength-dispersive spectrometer Panalytical Zetium, for determining bulk geochemical composition, with prior separate quantification of loss on ignition (LOI);
- Saturation and buoyancy weighing[45], for calculating open porosity, bulk and matrix density.

The results are summarized in Supplementary Fig. 1 together with information on each material's historical background—while the full XRF dataset is attached as Supplementary Data 3.

Field and laboratory simulations

Stone samples were prepared as 50 × 50 × 15 mm tiles with a plate of marine-grade 316 stainless steel attached on the side, providing a corrosion-resistant reference surface. For the field simulations, twenty-four specimens were assembled into three UES, each consisting of a cage-protected PVC

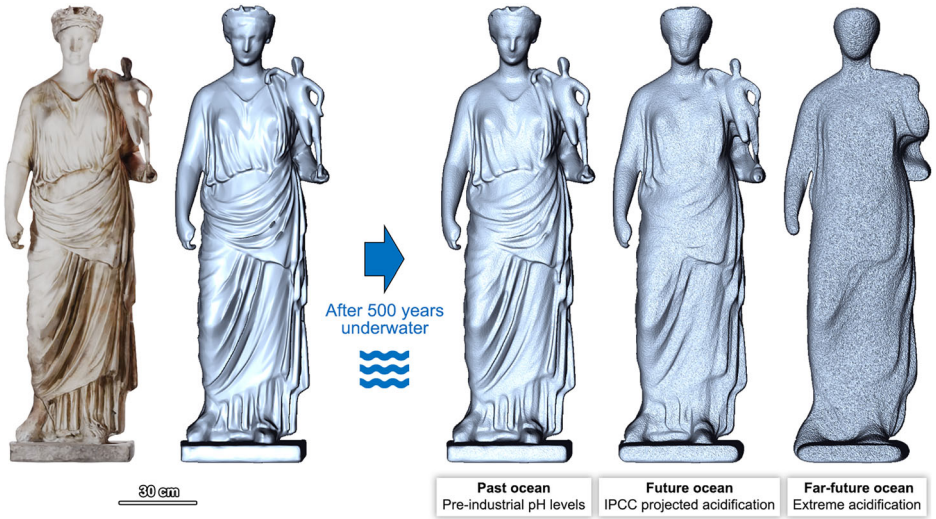

Fig. 5 | 3D simulations of archeological stone decay. Textured and untextured 3D model of the 1st-century AD marble sculpture portraying Antonia Minor, mother of Emperor Claudius, formerly underwater in the sunken Roman city of Baia and currently in the Archeological Museum of Campi Flegrei, Italy. The original mesh was digitally reshaped in Blender and Gwyddion, calibrating the elevation and roughness parameters based on the experimental data and their linear increase over time. Three different scenarios of underwater marble deterioration over 500 years were simulated at pH 8.2, 7.7, and 7.0, at 20 °C and shallow depth (original 3D model by 3D Research Srl, MUSAS project of Istituto Centrale per il Restauro, PON "Cultura e Sviluppo" FESR 2014–2020 funds).

mounting panel with fastenings for eight tiles, i.e., two for each different stone. For the laboratory simulations, twelve specimens were tested as is, three for each stone.

The underwater field experimentation was conducted at the island of Ischia, off the coast of Naples in southern Italy, an active volcanic area dotted with a number of natural submarine CO_2 seeps at different depths (Supplementary Fig. 3). The selection fell on the seeps along the southwestern shore of Aragonese Castle's islet (coordinates: 40.730683, 13.963273), which have served so far as an invaluable natural laboratory for ecology and climate change research and as an ocean acidification proxy[24,25]. The vents are located in shallow water and emit almost pure CO_2 (95%) at ambient seawater temperature (20 °C on average). There, the UES were installed in three locations within a distance of about 100 m, presenting a gradient of seawater pH controlled by the spatial variation of CO_2 venting intensity: ambient pH site (pH = 8.08 ± 0.07), acidification site (pH = 7.77 ± 0.32), and extreme acidification site (pH = 6.80 ± 0.43) (reference values from Foo et al.[24]). The depth was about 2 m for all UES. The installation took place in January 2023 and the monitoring lasted one year. Every four months, half of the specimens (one per stone type) for each UES were temporarily removed for the mid-term investigations and then reinstalled; the other half stayed underwater uninterruptedly until the end of the monitoring. Right after the sampling dives and prior to any mid-term or final analysis, the specimens collected were subjected to a bath in bleach (1–5% sodium hypochlorite solution with pH = 13), a manual cleaning of the metal reference surface, a rinse and bath in running water, and finally an oven drying at 70 °C. This routine allowed removing superficial salt residues and non-encrusting soft marine organisms. To that purpose, preliminary tests of mechanical cleaning and chemical cleaning with acetone, 36-volume hydrogen peroxide, and bleach were done; the last proved to be the best option for eliminating organic residues with no corrosion of the stone or the reference surface at the micrometric scale (also in line with Pingitore et al.[46]), color change apart.

The laboratory experimentation was conducted with a prototype enhanced environmental chamber, custom-made by FDM Environment Makers (Italy), which has been named MicroEnvironment Simulator (MES) (Supplementary Fig. 3). The MES was used for testing the materials immersed in filtered and sterilized seawater in controlled conditions, that is, with set temperature, pressure, and pH. Its main configuration consists of a 20-l 316-stainless-steel vessel with a temperature control jacket (0–100 °C), a set of charge/discharge pressure valves (0–10 bar) with gauge, and a pH control system for injecting CO_2, compressed air, or nitrogen, with associated temperature, pressure, and pH sensors, an electric mixer, and a charge/discharge water tank; the instrument is fully programmable and can be remotely controlled. The MES experimentation was conducted at a constant temperature of 20 °C (corresponding to recent averages of extra-polar ocean surface temperature[47]) and a gauge pressure of 1 bar (simulating shallow water depth), while varying pH (simulating ocean acidification); three tests were run, each lasting four months, at pH 8.20, 7.50, and 7.00, adjusted and kept constant by automatically injecting CO_2 or air. After each test, the stone specimens were extracted for the investigations and the seawater was replaced.

With this experimental outline, the field and laboratory tests allowed monitoring the stone materials by small-scale simulations of different ocean acidification scenarios, accounting for pre-industrial, present, and future seawater pH levels[3].

Seawater analysis

Seawater samples were collected at regular intervals from the three UES sites at the CO_2 vents, for acquiring pH measures and comparing them with the literature; however, since the natural pH gradient is highly variable, the reference values for this paper, as previously mentioned, derive from long monitoring periods and a data collection from different studies[24]. The measurements were done in situ right after sample collection with a portable pH-meter Mettler Toledo SevenGo SG2. Water temperature was also recorded with a dive computer. A second set of samples was filtered with 0.22-µm PES filters and refrigerated for subsequent chemical analyses: major ions were analyzed by ion chromatography, using a Dionex DX 500 system, and trace elements were analyzed by inductively coupled plasma mass spectrometry (ICP-MS), using an Agilent 7700× spectrometer. The properties directly measured are complemented by the data series provided by the local environmental monitoring agency ARPAC. Water samples were also collected after each MES test, following the same analytical routine. The datasets are included in Supplementary Data 4.

According to the results, the water samples analyzed in this study, all from the Tyrrhenian Sea (Italy), have a typical Mediterranean composition. Seawater at the UES sites exhibits seasonal variations, generally having higher salinity and levels of nutrients in winter (e.g., with sodium and chlorides increasing by about 10% compared to summer), with higher pH too (apart from the extreme acidification site). With regard to the seawater used for the MES tests, calcium concentration is higher (by up to 20%) when pH is lower, pointing out stronger calcite dissolution.

Quantification of stone decay

The changes occurred in the stone samples were investigated by monitoring their surface state evolution, that is, quantifying surface erosion/recession and any textural change involving roughness, surface area, etc.,

linked to dissolution processes. The morphometrics was based on the creation of high-resolution 3D models of the stone surfaces with a portable non-contact 3D optical profilometer Nanovea Jr25. Large mapping areas of 20 × 15 mm for all samples were selected to enhance statistical representativeness, including both the stone and the metal reference surface. For all the twenty-four UES specimens, their front surfaces and back surfaces (the latter fully in contact with the mounting panels) were both mapped, in order to get information on exposed areas with biofouling accumulation as well as on shielded areas with no biological growth; for half of the samples, the measurements were done at intermediate monitoring steps, as mentioned above. For the twelve MES specimens, only the front surfaces were mapped, at the end of each test. The profilometer is equipped with two optical pens providing a fixed vertical resolution of 3.4 and 41.0 nm within a z-measurement range of 1.4 and 24.0 mm, respectively; the lateral resolution (xy-step size) selected was 20 µm, with a scan speed of typically 6.43 mm/s (1000-1800 Hz dual-frequency acquisition) or anyway between 2.00 and 8.00 mm/s, depending on the sample characteristics. The 3D maps were processed with the software Gwyddion v2.67 (Czech Metrology Institute) by a three-step procedure: (1) image framing and correction and Laplace's interpolation of minor outliers; (2) leveling and rescaling, by subtracting the least-squares mean plane and setting the reference surface to zero; (3) microroughness filtering, by applying a conservative denoise filter and a Gaussian smoothing filter. The textural parameters of the stone surface and the differences in elevation between stone and reference surfaces were computed by an areal statistical analysis.

Finally, complementary investigations involved the sequential weighing of the MES specimens (after oven drying) for monitoring mass changes and the documentation of the biofouling on the UES specimens.

Data availability

The .xlsx files containing the datasets generated in this study are attached to this article as Supplementary Data and can also be accessed through a public online repository (https://doi.org/10.5281/zenodo.18002877).

Received: 5 August 2025; Accepted: 2 January 2026;
Published online: 16 January 2026

References

1. Gruber, N. et al. The oceanic sink for anthropogenic CO_2 from 1994 to 2007. *Science* **363**, 1193–1199 (2019).
2. IPCC *Climate Change 2023: Synthesis Report* (IPCC, 2023).
3. IPCC *Climate Change 2021: The Physical Science Basis* (Cambridge University Press, 2021).
4. von Schuckmann, K. et al. The state of the global ocean. In *8th edition of the Copernicus Ocean State Report (OSR8)* (eds von Schuckmann, K. et al.) Copernicus Publications, State Planet, 4-osr8, 1 (2024).
5. IPCC *The Ocean and Cryosphere in a Changing Climate: Special Report* (Cambridge University Press, 2019).
6. Widdicombe, S. et al. Unifying biological field observations to detect and compare ocean acidification impacts across marine species and ecosystems: what to monitor and why. *Ocean Sci.* **19**, 101–119 (2023).
7. Teixidó, N. et al. Functional changes across marine habitats due to ocean acidification. *Glob. Change Biol.* **30**, e17105 (2024).
8. IPCC *Climate Change 2022: Impacts, Adaptation and Vulnerability* (Cambridge University Press, 2022).
9. Leung, J. Y. S., Zhang, S. & Connell, S. D. Is ocean acidification really a threat to marine calcifiers? A systematic review and meta-analysis of 980+ studies spanning two decades. *Small* **18**, 2107407 (2022).
10. UNESCO *The UNESCO Convention on the Protection of the Underwater Cultural Heritage* (UNESCO, Paris, 2006).
11. Perez-Alvaro, E., Manders, M. & Underwood, C. Underwater cultural heritage in world heritage sites: figures and insights into possibilities and realities. *Hist. Environ. Policy Pract.* **15**, 611–643 (2025).
12. UNESCO *Convention on the Protection of the Underwater Cultural Heritage* (UNESCO, 2001).
13. IPCC *Climate Change 2014: Impacts, Adaptation, and Vulnerability. Part B: Regional Aspects* (Cambridge University Press, 2014).
14. Spalding, M. J. Perverse sea change: underwater cultural heritage in the ocean is facing chemical and physical changes. *Cult. Herit. Arts Rev.* **2**, 12–16 (2011).
15. Dunkley, M. 'Climate is what we expect, weather is what we get' – Managing the potential effects of oceanic climate change on underwater cultural heritage. In *Water & heritage: material, conceptual and spiritual connections* (eds Willems, W. J. H. & van Schaik, H. P. J.) 217–229 (Sidestone Press, 2015).
16. Perez-Alvaro, E. Climate change and underwater cultural heritage: impacts and challenges. *J. Cult. Herit.* **21**, 842–848 (2016).
17. Wright, J. Maritime archaeology and climate change: an invitation. *J. Marit. Archaeol.* **11**, 255–270 (2016).
18. Gregory, D. et al. Of time and tide: the complex impacts of climate change on coastal and underwater cultural heritage. *Antiquity* **96**, 1396–1411 (2022).
19. UNESCO *Climate Change and World Heritage* (UNESCO, Paris, 2007).
20. Orr, S. A., Richards, J. & Fatorić, S. Climate change and cultural heritage: a systematic literature review (2016–2020). *Hist. Environ. Policy Pract.* **12**, 434–477 (2021).
21. Sesana, E., Gagnon, A. S., Ciantelli, C., Cassar, J. & Hughes, J. J. Climate change impacts on cultural heritage: a literature review. *WIREs Clim. Change* **12**, e710 (2021).
22. Germinario, L. et al. Microclimate and weathering in cultural heritage: design of a monitoring apparatus for field exposure tests. *Heritage* **5**, 3211–3219 (2022).
23. Bonazza A. Sustainable heritage and climate change. In *Routledge Handbook of Sustainable Heritage* (eds Fouseki, K., Cassar, M., Dreyfuss, G. & Ang Kah Eng, K.) 263–271 (Routledge, 2023).
24. Foo, S. A., Byrne, M., Ricevuto, E. & Gambi, M. C. The carbon dioxide vents of Ischia, Italy, a natural system to assess impacts of ocean acidification on marine ecosystems: an overview of research and comparisons with other vent systems. In *Oceanography and Marine Biology: An annual review* (eds Hawkins, S. J., Evans, A. J., Dale, A. C., Firth, L. B. & Smith, I. P.) 56, 237–310 (CRC Press, 2018).
25. Teixidó, N. et al. Functional biodiversity loss along natural CO_2 gradients. *Nat. Commun.* **9**, 5149 (2018).
26. Naviaux, J. D. et al. Temperature dependence of calcite dissolution kinetics in seawater. *Geochim. Cosmochim. Acta*. **246**, 363–384 (2019).
27. Adkins, J. F. et al. The dissolution rate of $CaCO_3$ in the ocean. *Annu. Rev. Mar. Sci.* **13**, 57–80 (2021).
28. Feely, R. A. et al. In situ calcium carbonate dissolution in the Pacific Ocean. *Glob. Biogeochem. Cycles* **16**, 1144 (2002).
29. Larson, E. B. & Emmons, R. V. Dissolution of carbonate rocks in a laboratory setting: rates and textures. *Minerals* **11**, 605 (2021).
30. Salvini, S. et al. Recession rate of carbonate rocks used in cultural heritage: textural control assessed by accelerated ageing tests. *J. Cult. Herit.* **57**, 154–164 (2022).
31. Martínez-Martínez, J., Benavente, D., Pérez-Huerta, A., Cueto, N. & García-del-Cura, M. A. Changes on the surface properties of foliated marbles at different cutting orientations. *Constr. Build. Mater.* **222**, 493–499 (2019).
32. Fyfe, J., Fox-Kemper, B., Kopp, R. & Garner G. Data for Figure SPM.8 (v20210809), Summary for Policymakers, NERC EDS Centre for Environmental Data Analysis. In *Climate Change 2021: The Physical Science Basis*, IPCC (Cambridge University Press, 2021). https://doi.org/10.5285/98af2184e13e4b91893ab72f301790db.
33. Gutiérrez, J. M. et al. Atlas. In *Climate Change 2021: The Physical Science Basis*, IPCC, 1927–2058 (Cambridge University Press, 2021). http://interactive-atlas.ipcc.ch.

34. Hassoun, A. E. R. et al. Climate change risks on key open marine and coastal Mediterranean ecosystems. *Sci. Rep.* **15**, 24907 (2025).
35. Resetarits, H. M., Dishon, G., Agarwal, V. & Smith, J. E. The effects of temperature and CO_2 enrichment on the red seaweed *Asparagopsis taxiformis* from Southern California with implications for aquaculture. *J. Phycol.* **60**, 1567–1584 (2024).
36. Marchettoni, E., Germinario, L., Moschin, E., Mazzoli, C. & Moro, I. Effects of acidification on algal colonization and ecological succession on different carbonate substrates in the vent systems of the Castello Aragonese (Ischia Island, Italy). In *Italian Phycological Annual Meeting* (14–15 Nov 2025, Rome).
37. Schönberg, C. H. L., Fang, J. K. H., Carreiro-Silva, M., Tribollet, A. & Wisshak, M. Bioerosion: the other ocean acidification problem. *ICES J. Mar. Sci.* **74**, 895–925 (2017).
38. Caldeira, K. & Wickett, M. E. Ocean model predictions of chemistry changes from carbon dioxide emissions to the atmosphere and ocean. *J. Geophys. Res.* **110**, C09S04 (2005).
39. Hartin, C. A., Bond-Lamberty, B., Patel, P. & Mundra, A. Ocean acidification over the next three centuries using a simple global climate carbon-cycle model: projections and sensitivities. *Biogeosciences* **13**, 4329–4342 (2016).
40. Nicholls, R. J. et al. Stabilization of global temperature at 1.5 °C and 2.0 °C: implications for coastal areas. *Philos. Trans. R. Soc. A* **376**, 20160448 (2018).
41. Morse, J. W., Arvidson, R. S. & Lüttge, A. Calcium carbonate formation and dissolution. *Chem. Rev.* **107**, 342–381 (2007).
42. Hafner, A. & Underwood, C. J. Introduction to the impact of climate change on underwater cultural heritage and the decade of ocean science for sustainable development 2021–2030. In *Heritage Under Water at Risk: Threats – Challenges – Solutions* (eds Hafner, A., Öniz, H., Semaan, L. & Underwood, C. J.) 118–126 (ICOMOS, Paris, 2020).
43. Calvo, J. P. & Regueiro, M. Carbonate rocks in the Mediterranean region – from classical to innovative uses of building stone. In *Limestone in the Built Environment: Present-Day Challenges for the Preservation of the Past* (eds Smith, B. J., Gomez-Heras, M., Viles, H. A. & Cassar, J.) Special Publications, 331, 27–35 (Geological Society, 2010).
44. Siegesmund, S. & Török, Á. Building stones. In *Stone in architecture. Properties, durability* 5th edn (eds Siegesmund, S. & Snethlage, R.) 11–95 (Springer, 2015).
45. EN 1936 *Natural stone test methods - Determination of Real Density and Apparent Density, and of Total and Open Porosity* (CEN, Brussels, 2006).
46. Pingitore, N. E. et al. Dissolution kinetics of $CaCO_3$ in common laboratory solvents. *J. Sediment. Petrol.* **63**, 641–645 (1993).
47. Copernicus Climate Change Service *Global Climate Highlights 2024* (2025). https://climate.copernicus.eu/global-climate-highlights-2024.

Acknowledgements

This research is part of the project WATERISKULT, which has received funding from the European Union's Horizon 2020 research and innovation program under the Marie Skłodowska-Curie Individual Fellowships (grant agreement no. 101022386; awarded to Luigi Germinario). The authors thank the following people, institutions, and companies that supported this research by sharing their technical expertise and skills or helping with the provision of materials, data, and facilities: Abba Blu; ANS Diving Ischia; Castelli S., Ciervo B., Facciolo E., Marchettoni E., Moschin E., Paknazar B., Praticelli N., Sañudo Cox M.M., and the International Research Office (University of Padova); Capone S. (ARPAC); Chiarore A., Iacono B., Mirasole A., and Vigo Majello M.C. (Ischia Marine Center-SZN); Davidde B. (Istituto Centrale per il Restauro); Della Marca M. (FDM Environment Makers); Gallocchio E. (Parco Archeologico Campi Flegrei); G.B. Plast; Marine Protected Area "Regno di Nettuno"; Morrone D. and Rinaldi A. (Nanovea); Nečas D. (Brno University of Technology).

Author contributions

Conceptualization: L.G.; Formal analysis: L.G. and D.B.; Funding acquisition: L.G.; Investigation: L.G., M.M., I.M., D.B., F.T., and C.M.; Methodology: L.G. and M.M.; Project administration: L.G.; Resources: L.G., M.M., I.M., D.B., F.T., and C.M.; Supervision: C.M.; Validation: L.G. and D.B.; Visualization: L.G.; Writing—original draft: L.G.; Writing—review and editing: L.G., M.M., I.M., D.B., F.T., and C.M.

Competing interests

The authors declare no competing interests.

Additional information

Supplementary information The online version contains supplementary material available at https://doi.org/10.1038/s43247-026-03184-w.

Correspondence and requests for materials should be addressed to Luigi Germinario.

Peer review information *Communications Earth and Environment* thanks Beatriz Menéndez and Carlotta Sacco Perasso for their contribution to the peer review of this work. Primary handling editors: Christopher Cornwall and Alice Drinkwater. A peer review file is available.